Electronic structure of a bismuth bilayer

Christian R. Ast and Hartmut Höchst
Synchrotron Radiation Center, University of Wisconsin–Madison, Stoughton, Wisconsin 53589
(Received 15 November 2002; published 24 March 2003)

Using angle-resolved photoemission spectroscopy, we identified four two-dimensional bands within a 1 eV binding-energy region below the Fermi level. The top two bands that are part of the complex Fermi surface of Bi (111) are located in the projected bulk band gap and exhibit sixfold rotational symmetry of the top Bi bilayer. The two lower-lying bands reside inside the projected bulk band structure. The threefold rotational symmetry of these bands indicates a weak interaction with the underlying bulk bands. Our data can be explained with a tight-binding calculation of a bilayer by eliminating the second nearest-neighbor interactions that determine the coupling between bilayers in bulk Bi.

DOI: 10.1103/PhysRevB.67.113102 PACS number(s): 73.20.−r, 71.45.Lr, 73.25.+i, 79.60.−i

In recent years, the electronic properties of surfaces and layered materials have been a subject of extensive theoretical and experimental studies.[1–4] Commonly layered materials show a two-dimensional (2D) electronic structure with weak interlayer coupling in the bulk. The crystal structure of bismuth has a layered character, however, weak interlayer interactions induce a three-dimensional bulk band structure.[5] On the other hand, the topmost bilayer seems to be less bonded with the substrate due to the lack of translational symmetry along the surface normal. The reduced interaction with the underlying substrate confines electrons in the bilayer where they develop strong 2D electronic properties. Using synchrotron-radiation angle-resolved photoemission spectroscopy (ARPES) and variable photon energies, we have identified 2D states on Bi(111) that show behavior similar to surface states and surface resonances in which they only exist in the projected bulk band gaps or they follow the bulk dispersion, respectively.

Bismuth has rhombohedral (arsenic) crystal structure. Its space group is D_{3d}^5 $(R\bar{3}m)$ and the corresponding point group is D_{3d} $(\bar{3}m)$. It can be visualized as being composed of bilayers that are stacked in the (111) direction in *ABC* fashion. The bonds of the trivalent bismuth atoms are directed to the three nearest neighbors, which lie within the bilayer. Since there is only weak bonding between the bilayers, Bi single crystals cleave in the (111) plane. The integrity of the bilayer has been confirmed by scanning tunnel microscope measurements which show steps at the surface of heights commensurate with a bilayer.[6]

Unlike in the case of a (110) surface,[7] there are no dangling bonds at the (111) surface which leads us to propose that the 2D states originate from the topmost bilayer. The presence of the bilayer electronic structure is further supported by the fact that we have not observed a lifting of the spin degeneracy. The states also have the peculiar property that depending on the degree of localization in the bilayer they show sixfold or threefold rotational symmetry in the surface Brillouin zone (SBZ). These phenomena will be discussed in this paper.

The experiment was performed at the undulator Plane Grating Monochromator (PGM) beamline of the Synchrotron Radiation Center at the University of Wisconsin-Madison in Stoughton, Wisconsin.[8] First, we report a measurement of the elongated electron pocket of the 2D Fermi surface (FS) at $\bar{M}$. Measurements of the other parts of the Fermi surface can be found elsewhere.[9–11] A band-structure map through the long side of the electron pocket (band *A*) can be seen in Fig. 1(a). The red line shows the band dispersion $E(k)$ that was obtained by fitting Lorenzian line shapes (including Fermi function cutoff and Shirley background) to the energy distribution curves. We find a Fermi momentum of $k_F = 0.28$ Å^{-1} and an effective mass of about $1\,m_e$, seven times lower than previously reported.[11] A band-structure map through the thin part of the electron pocket (band *A*) can be seen in Fig. 1(b). It was taken parallel to the $\overline{\mathrm{K\,M\,K}}$ line at $k_y = 0.645$ Å^{-1} [see dashed blue line in Fig. 1(a)]. The peak appears as a very localized feature in energy as well as in momentum. The dispersion is so steep that the total width of the band is within the momentum resolution ($\Delta k = 0.032$ Å^{-1}) of the analyzer. Therefore, for this band, an estimate of the dispersion is shown as a red line. The band minimum is 22 meV and the Fermi momentum is $k_F = 0.007$ Å^{-1}. This yields an effective mass of $0.004\,m_e$. The aspect ratio of the electron pocket is 1:40.

Figure 2 shows a combination of band structure (BS) maps along $\overline{\Gamma\,\mathrm{M}}$ and along $\overline{\Gamma\,\mathrm{K}}$ displaying three bands (*A*, *B*, and *C*) that cross the Fermi level. The red lines show the fitted band dispersion $E(k)$. Near $\bar{\Gamma}$ and $\bar{\mathrm{M}}$, the emission intensity of these bands is greatly reduced. We have calculated the projected bulk BS of Bi from parameters of a third neighbor tight-binding (TB) calculation by Liu and Allen.[5] Their TB parameters are well suited for our needs since they have particularly focused on reproducing the minuscule bulk FS from experimental data. Figure 3(a) shows the Brillouin zones of the bulk and the (111) SBZ. The hatched area indicates the plane that was projected onto the $\overline{\Gamma\,\mathrm{M}}$ line. The projected bulk BS shown as the blue hatched area in Fig. 2 is localized near the Fermi level around the $\bar{\Gamma}$ and $\bar{\mathrm{M}}$ points because these bands cross the Fermi level near the *T* and *L* points. As one can see from Fig. 2, the 2D bands are limited in momentum space to the region of the projected bulk band gap. Thus, their behavior is similar to that of surface states.[4] A schematic of the 2D Fermi surface is shown in Fig. 3(b) displaying the sixfold rotational symmetry of the bands.

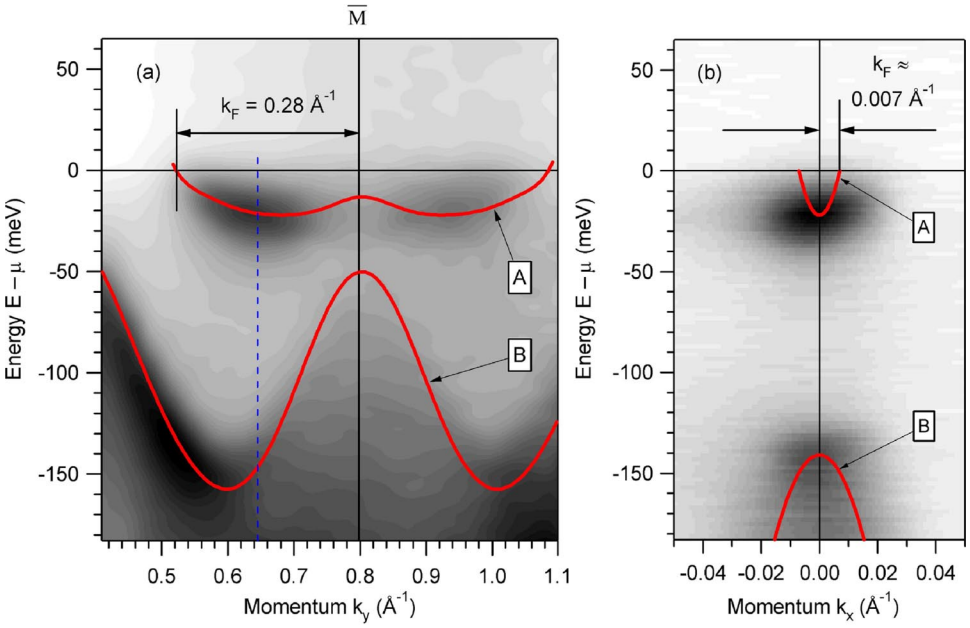

FIG. 1. (color online) ARPES intensity images of the electron pocket (band A) at $\bar{M}$. (a) Electron momentum $k_{||}$ along $\bar{\Gamma}\bar{M}$. (b) Electron momentum along a line parallel to $\bar{K}\bar{M}$ as indicated by the dashed blue line. The photon energy was 18 eV. The gray scale values vary linearly from white (zero intensity) to black (maximum intensity).

Two additional bands were observed at higher binding energies. Figure 4 shows band-structure maps obtained at two different photon energies. The two 2D bands D and E (green and yellow lines) can be easily identified by using variable photon energy. A 3D band F can be seen at a photon energy of 14 eV [see Fig. 4(a)] close to the Fermi level near the $\bar{\Gamma}$ point and rapidly dispersing downward. At a photon energy of 18 eV, the bulk band cannot be seen in the spectrum due to a gap in the final state. The projected bulk band structure is shown as a hatched area in the images. Both 2D states lie completely within the projected band structure. Their lifetime broadening is slightly larger than that of the 2D states located in the projected band gap. In the same energy range, previous experiments reported a 2D band that was interpreted as surface-state emission.[12–14] The band can be associated with band D but appears shifted in energy and/or momentum. In addition, they lack the details of the dispersion close to $\bar{\Gamma}$. These differences are most likely associated with small initial misalignments and coarse angular step widths.

A peculiar rotational symmetry behavior associated with the 2D states can be seen in Fig. 5. The image shows a band-structure image along a circular path in k space with radius $|k_{||}| = 0.25$ Å^{-1} and center at $\bar{\Gamma}$. The path is shown in a schematic of the Fermi surface. The angle α parametrizes the path in polar coordinates and is *not* to be confused with the angular coordinates of the analyzer. In polar coordinates, a sixfold or a threefold symmetric band has a period of 60° or 120°, respectively. Three 2D bands can be seen. The bands marked with a yellow (D) and a green (E) line correspond to the bands having surface resonance character and

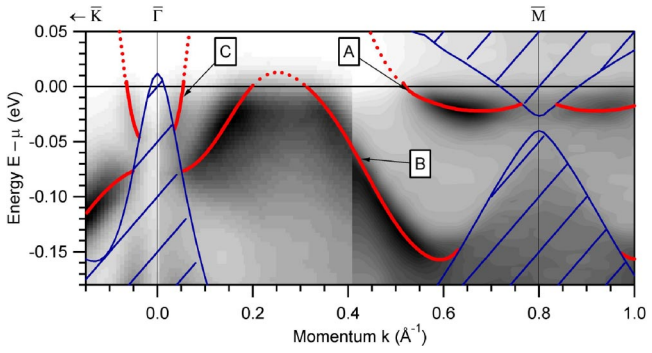

FIG. 2. (color online) Comparison of the ARPES band-structure image with the projected bulk band structure (hatched blue area) near the Fermi level. The image is assembled from three separate measurements along $\bar{\Gamma}\bar{K}$ and $\bar{\Gamma}\bar{M}$. The red lines indicate the band dispersion. The emission from these bands is clearly restricted to the energy-gap region outlined by the projected bulk band structure. The photon energy was 18 eV. The gray scale values vary linearly from white (zero intensity) to black (maximum intensity).

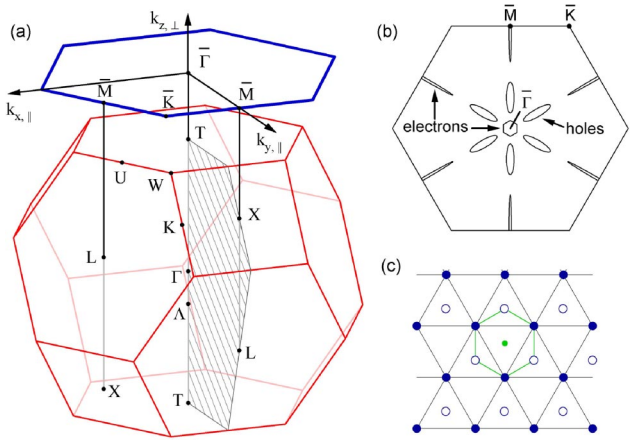

FIG. 3. (color online) (a) Bulk (red) and surface (blue) Brillouin zone of Bi(111). (b) Schematic of the various 2D-Fermi-surface segments in Bi(111). (c) Schematic of Bi bilayer structure. Open circles are above the paper plane, filled circles denote lattice points below the plane.

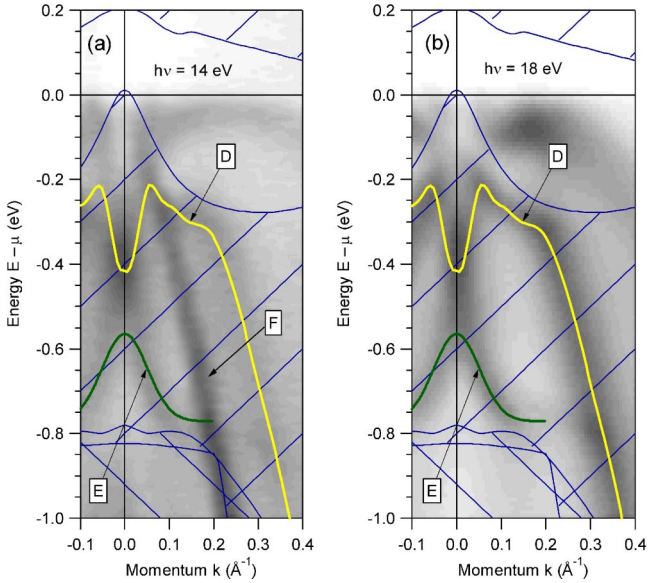

FIG. 4. (color online) Comparison of ARPES intensity image near $\bar{\Gamma}$ with the projected bulk band structure at different photon energies. The electron momentum $k_{||}$ is along $\bar{\Gamma}\bar{M}$. (a) $h\nu = 14$ eV; the dispersion of the 2D bands *D* and *E* (yellow and green lines) does not depend on photon energy. Band *D* follows the dispersion of the bulk band *F*. (b) $h\nu = 18$ eV; the bulk band (*F*) emission is suppressed due to a gap in the final state. The gray scale values vary linearly from white (zero intensity) to black (maximum intensity).

show threefold rotational symmetry. The band marked with a red line (*B*) having surface-state character shows sixfold symmetry. The sixfold symmetry of band *C* has been discussed elsewhere.[15]

Figure 3(c) shows a schematic of a single bilayer in bismuth. The open and filled circles represent lattice sites of the bilayer shifted by a distance *z* above and below the paper plane, respectively. Upon inspection, a threefold rotational axis (perpendicular to the paper plane) and three vertical mirror planes can be identified. This corresponds to the point group C_{3v}. In addition, the bilayer has space inversion symmetry C_i. Combining these two symmetry groups, we have $D_{3d} = C_{3v} \otimes C_i$ which is the same point group as the bulk.[16,17] In momentum space, the bilayer clearly yields a hexagonal 2D Brillouin zone and the energy bands still have to transform into themselves under all symmetry operations of the lattice. This has to result in sixfold symmetric energy bands as can be seen in the following example. The symmetry operation S_6, which is composed of a rotation by 60°

TABLE I. Tight-binding parameters used in the calculation of a Bi bilayer. The nomenclature was adopted from Liu and Allen (Ref. 4). Unprimed and double primed parameters refer to bonds between nearest and third nearest neighbors in the bulk. Single primed parameters consider the interaction of atoms between two bilayers.

E_s	−1.166	$V_{pp\sigma}$	0.6	$V'_{pp\sigma}$	0	$V''_{pp\sigma}$	0.087
E_p	−0.432	$V_{pp\pi}$	−0.236	$V'_{pp\pi}$	0	$V''_{pp\pi}$	0.021
$V_{ss\sigma}$	0.413	$V'_{ss\sigma}$	0	$V''_{ss\sigma}$	−0.317	λ	0.2
$V_{sp\sigma}$	0.396	$V'_{sp\sigma}$	0	$V''_{sp\sigma}$	0.518		

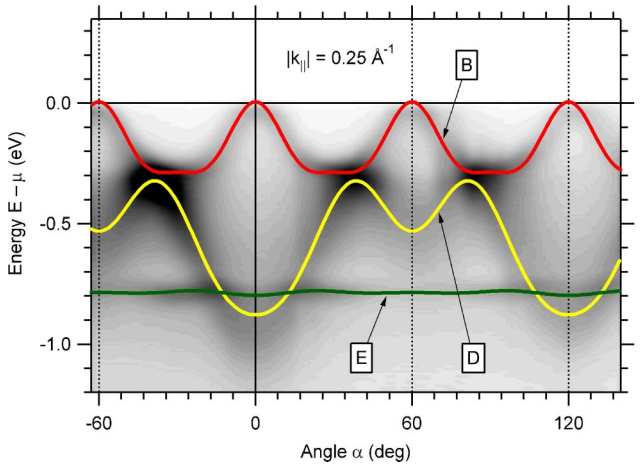

FIG. 5. (color online) ARPES intensity image along a circular momentum path at $|k_{||}| = 0.25$ Å^{-1}. At this momentum, the image cuts through the 2D bands *B* (red), *D* (yellow), and *E* (green). Band *B* exhibits the sixfold rotational symmetry of the surface Brillouin zone, while bands *D* and *E* couple with bulk states and are threefold symmetric.

followed by a reflection through a plane perpendicular to the axis of rotation, reduces to C_6, a rotation by 60°, because the following reflection has no effect in two dimensions. We conclude from the sixfold symmetry of the bands *A*, *B*, and *C* that the states in these bands are localized in the bilayer, whereas the states of the threefold symmetric bands *D* and *E* penetrate into the bulk. This is in agreement with their resemblance to a surface state or surface resonance, respectively.

Space inversion symmetry requires the energy bands to transform as $E(\vec{k},\uparrow) = E(-\vec{k},\uparrow)$, where ↑ and ↓ denote the spin state. Combining this with time-reversal symmetry $E(\vec{k},\uparrow) = E(-\vec{k},\downarrow)$, we find $E(\vec{k},\uparrow) = E(\vec{k},\downarrow)$ which results in spin degeneracy. The sixfold symmetry of bands *A*, *B*, and *C* is a clear indication that potential asymmetries in the bilayer due to the surface can be ruled out and inversion symmetry holds. If the spin degeneracy were lifted, the effect would clearly be visible since spin-orbit coupling is about three times stronger in Bi (1.5 eV) than in Au (0.47 eV).[18,19] In addition, the bands would still have to be degenerate at high-symmetry points $[E(0,\uparrow) = E(0,\downarrow)]$, which we do not observe either. Thus, the experimental findings suggest that the bands are spin degenerate.

The photoemission intensity from the 2D bands are rather insensitive to ultrahigh vacuum surface contamination. In addition, attempts to gradually quench the 2D emission by decorating the surface with Au failed but showed the strong tendency of Bi atoms to float, a Bi property frequently utilized in surfactant-mediated epitaxy.[20–22]

It was previously reported that sheet densities did not include the electron pocket at $\bar{M}$.[9] Including the pocket we find hole and electron sheet densities of $p_s = 1.1 \times 10^{13}$ cm^{-2} and $n_s = 1.5 \times 10^{13}$ cm^{-2}, respectively, which is, considering the uncertainty in the estimates at $\bar{M}$, close to charge neutrality. Assuming charge neutrality for the 2D electronic structure, we find a similar situation as in the bulk: A band overlap —

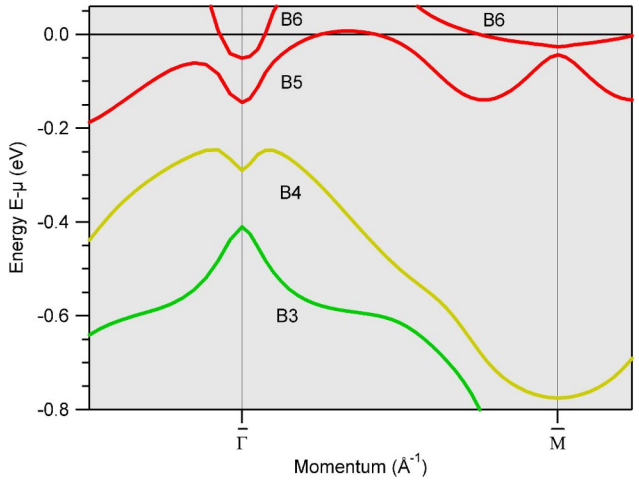

FIG. 6. (color online) Tight-binding band structure of a Bi bilayer. The dispersion and symmetry of bands $B5$, $B6$ closely match the bands A, B, and C in Fig. 2. The dispersion of bands $B3$, $B4$ at $\bar{\Gamma}$ resembles the bands D and E in Fig. 4. The two lower-lying ''s-like'' bands $B1$, $B2$ are not shown.

indirect negative band gap with minimum at L and maximum at T — leads to ''spilling'' electrons from the otherwise completely filled valence band into the conduction band resulting in metallic behavior (see Fig. 2). This scenario requires an even number of electrons per primitive cell which can only be provided by a bilayer since it has two Bi atoms in the basis. Furthermore, Betti *et al.* showed that Bi films grown epitaxially on InAs become metallic at a layer thickness of two monolayers, while thinner films are semiconducting.[23]

Using the tight-binding parametrized equations by Liu and Allen,[5] we have performed a band-structure calculation of the bilayer. The Bi bilayer was simulated by simply setting the second nearest-neighbor tight-binding parameters to zero such that interactions are restricted to nearest and third nearest neighbors. The parameters entering the calculation are given in Table I. Figure 6 shows the relevant section of the calculated layer band structure. As one can see, the band structure closely resembles our experimental findings. The Fermi surface is also well reproduced by our calculations. For the purpose of the present paper, we wanted to replicate the basic overall features of the bilayer band structure and accompanying 2D Fermi surface by varying a minimal subset of the tight-binding parameters. The most noticeable difference compared to the bulk parameters is the need to increase the bilayer thickness from 1.59 Å to 2.72 Å and decrease the spin-orbit coupling λ from 1.5 eV to 0.2 eV. Without these changes, the Fermi surface would contain additional segments not seen in the experimental data. The change in bilayer thickness is the only degree of freedom in a surface relaxation because low-energy electron diffraction shows a nonreconstructed pattern.[24] The two lower-lying ''s-like'' bands predicted by the calculation are harder to observe since they coincide with bulk bands, which makes the analysis more difficult.

Our observations (crystal properties, symmetry observations, spin degeneracy, band filling, insensitivity to surface contamination, as well as band-structure calculations) cannot be associated with *bona fide* surface states but strongly support the existence of a 2D electronic structure originating in the topmost bilayer of Bi(111).

We thank D. L. Huber for valuable discussions. The Synchrotron Radiation Center (SRC) is funded by the National Science Foundation (NSF) under Grant No. DMR-0084402.

[1] E.W. Plummer *et al.*, Surf. Sci. **500**, 1 (2002), and references therein.
[2] M.A.H. Vozmediano, M.P. López-Sancho, and F. Guinea, Phys. Rev. Lett. **89**, 166401 (2002).
[3] T. Valla *et al.*, Nature (London) **417**, 627 (2002).
[4] N. Memmel, Surf. Sci. Rep. **32**, 91 (1998).
[5] Y. Liu and R.E. Allen, Phys. Rev. B **52**, 1566 (1995).
[6] A.M. Troyanovskii and V.S. Edelman, Crystallogr. Rep. **44**, 300 (1997).
[7] S. Agergaard *et al.*, New J. Phys. **3**, 15 (2001).
[8] The total-energy resolution (photon plus electron) is 25 meV. The angular resolution was 1°. Bi single-crystal samples were cleaved *in situ* and kept at a pressure of $<8\times10^{-11}$ Torr. The sample temperature was set to 50 K in order to minimize phonon related broadening effects (the Debye Temperature of Bi is 120 K).
[9] C.R. Ast and H. Höchst, Phys. Rev. Lett. **87**, 177602 (2001).
[10] C.R. Ast and H. Höchst, Phys. Rev. B **66**, 125103 (2002).
[11] M. Hengsberger *et al.*, Eur. Phys. J. B **17**, 603 (2000).
[12] F. Patthey, W.-D. Schneider, and H. Micklitz, Phys. Rev. B **49**, 11 293 (1994).
[13] J. Thomas, G. Jezequel, and I. Pollini, J. Phys.: Condens. Matter **11**, 9571 (1999).
[14] A. Tanaka *et al.*, Phys. Rev. B **59**, 1786 (1999).
[15] C.R. Ast and H. Höchst, Phys. Rev. Lett. **90**, 016403 (2003).
[16] G. Burns, *Introduction to Group Theory with Applications* (Academic Press, Orlando, 1977).
[17] G. F. Koster, in *Solid State Physics*, edited by F. Seitz and D. Turnbull (Academic Press, New York, 1957), Vol. 5.
[18] F. Reinert *et al.*, Phys. Rev. B **63**, 115415 (2001).
[19] S. LaShell, B.A. McDougall, and E. Jensen, Phys. Rev. Lett. **77**, 3419 (1996).
[20] T. Schmidt *et al.*, Appl. Phys. Lett. **74**, 1391 (1999).
[21] B.N. Zvonkov *et al.*, Nanotechnology **11**, 221 (2000).
[22] S.W. Jun *et al.*, J. Cryst. Growth **235**, 15 (2002).
[23] M.G. Betti *et al.*, Phys. Rev. B **58**, R4231 (1998).
[24] F. Jona, Surf. Sci. **8**, 57 (1967).